Inorganic Chemistry

Article

pubs.acs.org/IC

Metal Ions as Cofactors for Aggregation of Therapeutic Peptide Salmon Calcitonin

Neeraj Rastogi,[†] Kalyan Mitra,[‡] Dinesh Kumar,[†] and Raja Roy*[,†]

[†]Centre of Biomedical Magnetic Resonance, Sanjay Gandhi Postgraduate Institute of Medical Sciences Campus, Lucknow 226014, India

[‡]E. M. Unit, Central Drug Research Institute, CSIR, Lucknow 226001, India

Supporting Information

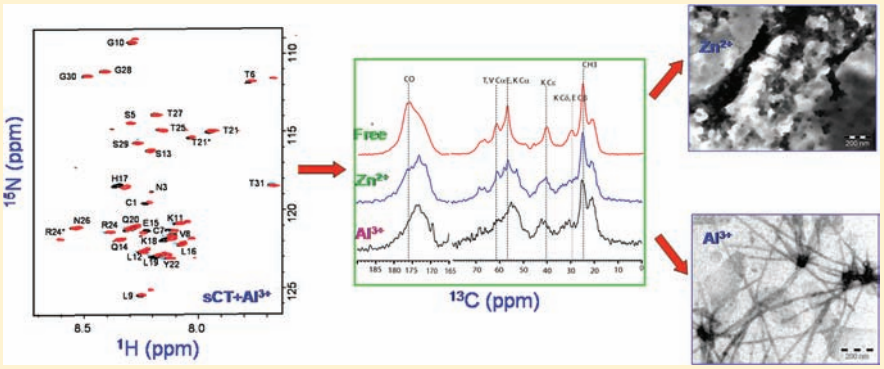

ABSTRACT: The effects of multivalent metal ions ($Cu^{2+}/Zn^{2+}/Al^{3+}$) on the aggregation of salmon calcitonin (sCT)—a therapeutic peptide used worldwide in the treatment of osteoporosis and Paget's disease—have been studied *in vitro* using NMR (both solution state and solid state), TEM, ThT-fluorescence, and FT-IR spectroscopy. Overall, the various results indicated that the metal-ions-induced conformational transitions in the peptide—mostly toward the β-sheet—facilitate the aggregation of sCT in solution. First, the solution NMR has been used to check the interaction between the peptide and the metal ions. Following this, the formation and characterization of calcitonin aggregates has been performed using TEM, solid state NMR, and FT-IR spectroscopy. The TEM and ThT-fluorescence results revealed that the sCT peptide incubated with Cu^{2+} and Zn^{2+} metal ions (in aqueous environment) forms globular aggregates, while that with Al^{3+} ions forms fibrils. The solid state NMR and FT-IR studies revealed the presence of a substantial amount of β-sheet content in sCT aggregates (formed in the presence of these metal ions) compared to the monomeric sCT, indicating that the metal binding is concomitant with conformational changes. The present study becomes crucial while prescribing this drug peptide under physio-pathological conditions associated with an abnormal accumulation of metal ions ($Cu^{2+}/Zn^{2+}/Al^{3+}$) in the body (i.e., abnormal metal ion homeostasis).

INTRODUCTION

Peptides have been extensively utilized in therapeutic formulations due to their participation in various metabolic pathways. Their capability to act as a drug is confined to a particular conformation and is lost on conformational transition. Therefore, it is important to determine the factors which facilitate such conformational alterations leading to a decrease in the efficacy of these therapeutic peptides. The study in turn will help to guide the use of these drug peptides under various physio-pathological conditions.

Calcitonin—a peptidal hormone which regulates the calcium−phosphorus metabolism in our body[1,2]—is one such type of peptide used in the treatment of metabolic bone disorders resulting due to altered calcium−phosphorus metabolism[1] like osteoporosis, Paget's disease, hypercalcemia of malignancy, and musculoskeletal pain.[3−6] For curing these diseased states, synthetic or recombinant human calcitonin (hCT) and salmon calcitonin (sCT) are generally used. However, hCT is not a widely used preparation in clinical practice because of its extremely high tendency to aggregate in the form of amyloid fibrils, resulting in cytotoxicity (as has been reported in several *in vitro* studies).[5,7−10] A well-known example is "Etiopathology of Human Medullary Thyroid Carcinoma," which is a consequence of amyloid fibril formation tendency exhibited by human calcitonin.[11] The disease is associated with amyloid fibrils deposited in the thyroid and adjacent enlarged lymph nodes.[11] Moreover, the hCT aggregates have been found to be comparatively more neurotoxic as compared to that of well-known amyloidogenic peptides (such as β-amyloid, α-synuclein, and prion proteins).[11] Aggregation not only creates a serious problem during production, storage, and administration of hCT but it can also lead to a significant decrease in its activity as a drug.[12] This

Received: December 3, 2011
Published: May 9, 2012

   dx.doi.org/10.1021/ic202604v | *Inorg. Chem.* 2012, 51, 5642−5650

Table 1. Acquisition Parameters Used to Acquire the Various ^{15}N Edited TOCSY and NOESY Experiments on Uniformly ^{15}N Labeled Peptide Salmon Calcitonin

parameters (rat nNOS fragment)	$^{1}H-^{15}N$ HSQC Or (SOFAST HMQC)	3D-TOCSY HSQC	3D-NOESY HSQC	3D-HMQC-NOESY-HSQC
complex data points	1024 × 128 (^{1}H, ^{15}N)	1024 × 72 × 200(^{1}H, ^{15}N, ^{1}H)	1024 × 72 × 200 (^{1}H, ^{15}N, ^{1}H)	1024 × 72 × 72 (^{1}H, ^{15}N, ^{1}H)
no. of scans per FID	16	16	16	16
recycling delay (t_{rec})	1 s (0.4 s)	1.5 s	0.8 s	0.8
spectral widths (ppm)	SW(^{1}H) = 10, SW(^{15}N) =20	SW(^{1}H) = 10, SW(^{15}N) = 20, SW(^{1}H) = 10	SW(^{1}H) = 10, SW(^{15}N) = 20, SW(^{1}H) = 10	SW(^{1}H) = 10, SW(^{15}N) = 20, SW(^{15}N) = 20
carrier frequencies (ppm)	O(^{1}H) = 4.7, O(^{15}N) = 117.5	O(^{1}H) = 4.7, O(^{15}N) = 117.5	O(^{1}H) = 4.7, O(^{15}N) = 117.5	O(^{1}H) = 4.7, O(^{15}N) = 117.5
mixing time		100 ms	400 ms	400 ms

is the reason that salmon calcitonin (sCT) has been the clinically preferred alternative to hCT for several years despite its low sequence identity (~50%). Lower aggregation propensity is further supported by the higher conformational stability of sCT in solution compared to hCT.[10] Further, sCT has 40−50 times higher intrinsic potency when compared to human calcitonin.[13] However, several *in vitro* studies[3,14,15] have also shown that sCT does exhibit a finite tendency to form aggregates in an aqueous environment, which limits its effectiveness as a drug, mainly because the aggregates, in addition to their cytotoxic effect, have a tendency to stimulate undesirable immune responses or severe allergic reactions. Therefore, it is highly important to investigate and define the factors driving the aggregation of sCT in solution, as it is still the most potent of the calcitonin preparations available, clinically most effective, and well tolerated. The information becomes crucial while prescribing this drug under physiopathological conditions associated with an abnormal accumulation of metal ions (Cu^{2+}/Zn^{2+}/Al^{3+}) in the body (i.e., abnormal metal ion homeostasis).

Several *in vitro* studies have shown that most proteins that undergo aggregation exhibit a high degree of conformational instability in which various regions of the polypeptide chain undergo noncooperative conformational changes.[16] The conformational instability has also been reported in the sCT peptide in an aqueous environment.[10,17,18] However, in most such cases, the aggregation does not take place until and unless some particular cofactor is involved, inducing destructive conformational transition; e.g., aggregation of amyloidogenic peptides (such as β-amyloid in the case of AD, α-sinuclein in Parkinson's disease, and prion protein in Prion's disease) is dependent on various environmental factors such as temperature, pH, and the presence of metal ions.[19,20] Among all of these cofactors, metal ion dys-homeostasis has been found to be the most common factor responsible for aggregation of these amyloidogenic peptides.[16] Though metal ions play a critical role in maintaining the correct conformations of a number of proteins inside the body,[21] these metal ions (Cu^{2+}, Mn^{2+}, Zn^{2+} and Al^{3+}) however have also been reported facilitating the aggregation of amyloidogenic peptides via inducing destructive conformational transitions.[22−28] Thus, they play an important role in the etiopathogenesis of several neurodegenerative disorders. The pro-aggregation effects are generally mediated through metal binding to proteins followed by small conformational changes in these proteins.[23] For example, endogenous "biometals" such as Cu^{2+} and Zn^{2+} have been probed to trigger the aggregation of human prion protein[24,28−32] and β-amyloid peptide.[33] Moreover, Zn^{2+} has also been found to involved in oligomerization of the peptide hIAPP, as in case of type II diabetes.[34,35] The consequences of metal ion dys-homeostasis on the aggregation of amyloid-β peptide as well as on hIAPP have been extensively reviewed.[36,37] Further, exogenous ones such as aluminum (Al^{3+}) have also been shown to play a crucial role in the aggregation of β-amyloid peptide.[22]

Several cofactors (like pH, temperature, and solvent) have been reported to be associated with the aggregation of calcitonin.[14] In addition to these cofactors, hydroxy radicals [$^{\bullet}OH$] and hydrogen peroxide [H_2O_2] have also been reported as cofactors in accelerating calcitonin aggregation.[7] In a very recent study, the role of concentration on the conformational transition of human calcitonin leading to its aggregation has been investigated using detailed NMR and TEM studies.[38] However, to the best of our knowledge, no work has been reported on the interaction of metal ions with calcitonin (both hCT as well as sCT) and their consequences on its self-association propensity. Interestingly, like salmon calcitonin, most of the amyloidogenic peptides/proteins have been reported to be natively disordered.[39] This prompted us to study the effect of metal ions (Cu^{2+}/Zn^{2+}/Al^{3+}) on such an important peptide because of its high therapeutic importance. The study will be very helpful in understanding the molecular basis of metal-ion-induced aggregation of the sCT peptide and thus will help to guide (i) the rational designing of robust aggregation-resistant bioactive sCT analogues and (ii) the design of a robust matrix for the controlled release of bioactive calcitonin.

MATERIALS AND METHODS

Sample Preparation. The peptide—salmon calcitonin in powder form—for carrying out the study was gifted by Sun Pharma Advance Research Company Ltd., Baroda, Gujrat (India), where it was synthesized through the solid phase synthesis method. The mass of the peptide was further confirmed by MALDI TOF ESI-MS. However, for backbone amide assignment, the ^{15}N-labeled peptide has been purchased from CIRMMP Italy: http://www.cerm.unifi.it/about-cerm/cirmmp. Reagent grade zinc chloride ($ZnCl_2$), copper chloride ($CuCl_2{\cdot}2H_2O$), and aluminum sulfate [$Al_2(SO_4)_3{\cdot}16H_2O$] of ≥98% purity were purchased from Merck Chemicals (www.merck-chemicals.com). Throughout the study, peptide solutions prepared in purified water (Milli-Q, Millipore) were used. The final pH of each sample solution was adjusted to 6.5 (suitable both for NMR as well as for mimicking near physiological conditions) using dilute HCl (reagent grade from Merck).

NMR Spectroscopy, Data Acquisition, and Analysis. All of the solution state NMR experiments have been performed on a Bruker Avance III 800 MHz spectrometer equipped with triple resonance cryoprobe. To see the effect of metal ions on the peptide in aqueous solution, 1D ^{1}H NMR spectroscopy has been used. 1D ^{1}H NMR experiments were performed on sCT samples (each 0.25 mM in concentration, pH ~ 6.5) prepared in purified water (90% H_2O + 10% D_2O). To induce the aggregation, each of these samples was incubated for 10 days with equimolar $CuCl_2$, $ZnCl_2$, and $Al_2(SO_4)_3$ with constant

dx.doi.org/10.1021/ic202604v | Inorg. Chem. 2012, 51, 5642−5650

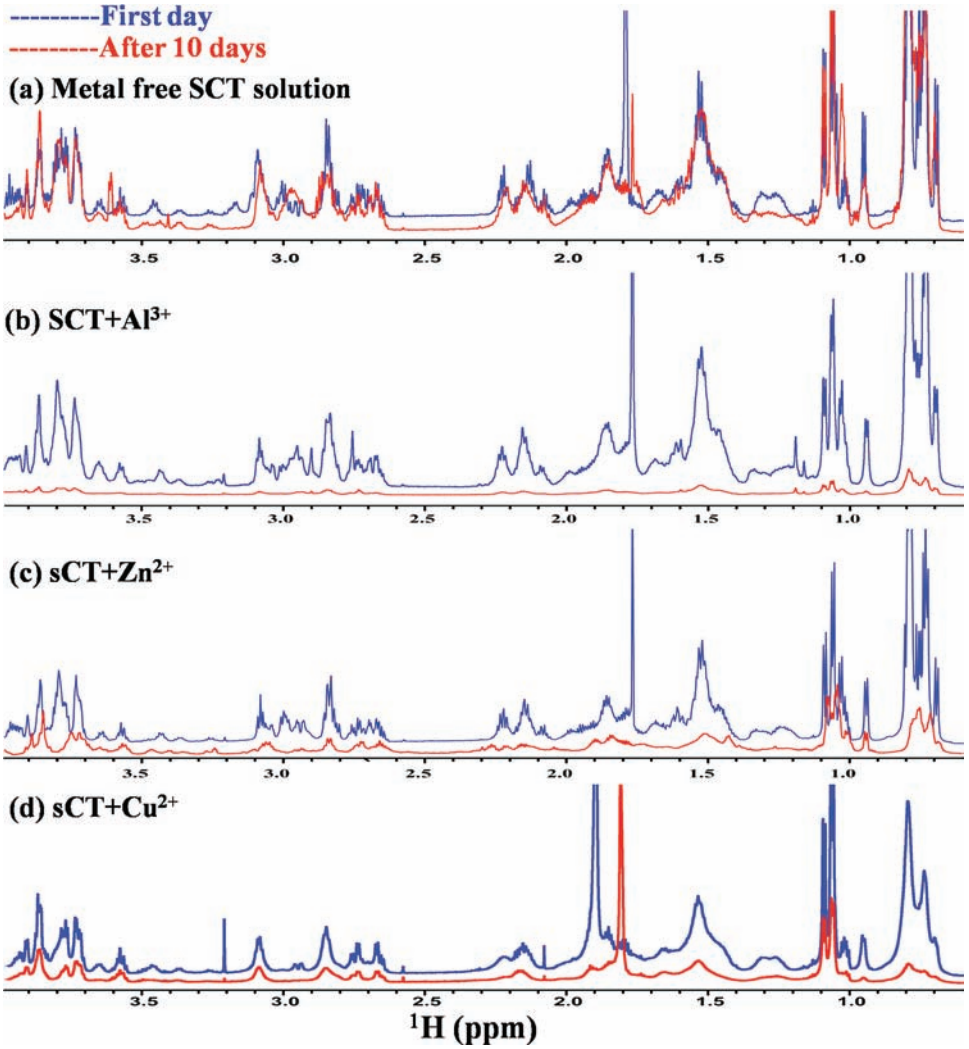

Figure 1. Overlaid 1D ^{1}H NMR spectra of the aliphatic region of sCT solutions the first day and after incubation for 10 days with agitation at 37 °C in the absence (a) as well as in the presence of (b) Al^{3+}, (c) Zn^{2+}, and (d) Cu^{2+} ions.

agitation at 37 °C and 250 rpm. To rule out the possibility of peptide aggregation because of agitation at 37 °C, a metal-free control sCT sample (in deionized water and 0.25 mM in concentration) was also incubated for 10 days. To check the aggregation, a series of 1D ^{1}H NMR spectra were recorded, first just after the addition of metal ions in the sCT peptide solutions and then after every day in-between the agitation process with metal ions. For better water suppression, the excitation sculpting pulse sequence was used. Spectral parameters for these experiments are as follows: relaxation delay, 2 s; number of scans, 32 with 32 000 data points.

Next, to gain the residue level information about the metal ion binding to sCT, the chemical shift perturbation method was used. For this, first, the assignment of backbone amide resonances of the sCT peptide in aqueous solution was determined using ^{15}N labeled peptide (~1 mM in concentration, pH = 6.5, temperature = 298 K) following a strategy (described in Appendix I of the Supporting Information with the help of Figures S2−S6) based on ^{15}N edited TOCSY and NOESY experiments, e.g., 3D TOCSY-HSQC (Figure S2), 3D NOESY-HSQC, and 3D HMQC-NOESY-HSQC (Figure S3).[40] The various acquisition parameters used for recording these experiments are given in Table 1.

All the spectra were processed using Topspin-2.1 (BRUKER, http://www.bruker.com/) and analyzed using CARA.[41] Prior to Fourier transformation and zero-filling, data were apodized with a sine-squared weighting function shifted by 60° along each dimension.

Following the backbone amide assignment, the interaction between metal ions (Cu^{2+}, Zn^{2+}, and Al^{3+}) and the sCT peptide was investigated based on amide chemical shift perturbation. Four peptide samples were prepared (each 1 mM in concentration, pH 6.5) and subjected to incubation at 37 °C for 2 h: one sample without any metal ion and the other three samples with 1 equivalent of $CuCl_2$, $ZnCl_2$, and $Al_2(SO_4)_3$. After incubating for about 2 h, 2D ^{1}H−^{15}N SOFAST-HMQC spectra[39,42] were recorded for each sample in order to investigate interaction-induced changes in the amide −NH resonances. In order to ascertain the chemical shift perturbation results as a phenomenon of solely coordination between metal ions and peptide, the previous peptide samples (1 mM in concentration, pH ~ 6.5) containing Cu^{2+} and Zn^{2+} metal ions were incubated further with 2 equivalents of EDTA at 37 °C for 2 h. After incubation, the SOFAST-HMQC spectra were recorded for both the EDTA treated peptide samples.

Transmission Electron Microscopy. For TEM analysis, a 7 μL sample was deposited on glow discharged pioloform-coated copper grids and allowed to adsorb for 2 min. Excess solution was blotted off using filter paper. The grids were then washed with triple distilled water and negatively stained with 1% phosphotungstic acid (pH adjusted to 7) and air-dried. Grids were analyzed under a Philips FEI Tecnai 12 Twin Transmission Electron Microscope at 80 kV after complete gun alignment and astigmatism corrections. Images were acquired at magnifications ranging from 11 000× to 52 000× using a

dx.doi.org/10.1021/ic202604v | Inorg. Chem. 2012, 51, 5642−5650

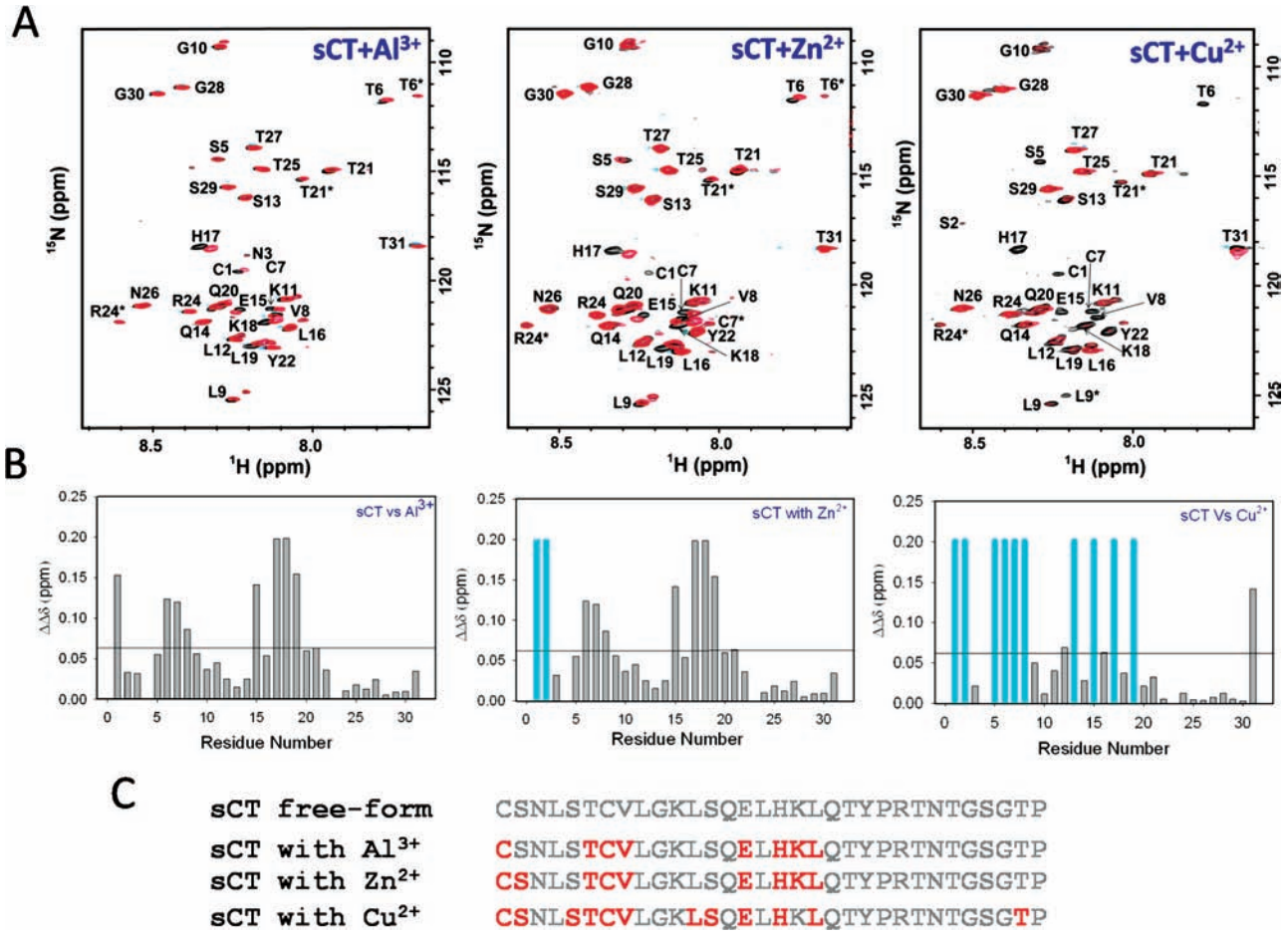

Figure 2. (A) $^{1}H-^{15}N$ HMQC overlaid spectra of sCT incubated with 1 equivalent of Al^{3+}, Zn^{2+}, and Cu^{2+} for 2 h at 37 °C and pH 6.5. Black peaks here are from metal free sCT, while red ones are from that in the presence of metal ions. (B) Residue-wise average combined chemical shift perturbations (defined as $\Delta\delta_{ppm} = [(5*\Delta\delta_H)^2 + (\Delta\delta_N)^2]^{1/2}$) in the presence of metal ions plotted as a function of the amino acid sequence of sCT. The residues whose resonances disappear in the presence of metal ions are shown in cyan. (C) The residues undergoing chemical shift perturbations in $^{1}H-^{15}N$ HMQC are mapped in red on the primary sequence of the peptide.

MegaView ll CCD camera and analyzed using analySIS software. At least eight grids were prepared and analyzed for each sample.

FT-IR Spectroscopy. The secondary structural components present in monomeric and aggregated forms of sCT were investigated using FT-IR spectroscopy. The aged samples with metal ions were lyophilized to obtain aggregated peptide in the solid form. The monomeric and aggregated sCT pellets were obtained by mixing each of these samples (in solid state) with KBr. The KBr-peptide pellets were then used for infrared spectroscopy on a Thermo Nikolet Nexus FT-IR spectrometer, using 16 scans, and were reported in cm^{-1}.

ThT Fluorescence Measurements. Thioflavin T (ThT) fluorescence assays were measured with a Perkin-Elmer LS 55 fluorescence spectrometer with an excitation wavelength of 445 nm and an emission range from 460 nm to 560 nm at 37 °C. To observe the changes in the emission fluorescence of ThT, the sCT solutions incubated for 10 days in the presence as well as in the absence of metal ions (in a final concentration of 25 μM) were mixed with 10 μM ThT in aqueous solution.

Solid State NMR Study. High-resolution solid-state ^{13}C NMR spectroscopy has proven to be a powerful tool for monitoring the secondary structural changes in proteins incurred during transition from the monomeric to the aggregate state.[43] The peptide solutions incubated (for 10 days at 37 °C) with metal ions (here Zn^{2+} and Al^{3+}) were dialyzed first in order to remove the excessive metal ions, and then these dialyzed samples were subjected to lyophilization in order to get the aggregates in the solid form to perform solid state NMR experiments. All of the solid state NMR experiments were performed on a 600 MHz NMR spectrometer (corresponding to a magnetic field strength of 14.1 T) equipped with a 3.2 mm double variable temperature (DVT) magic angle spinning (MAS) probe (Bruker Biospin, Germany). For solid state NMR experiments, monomeric and aggregated peptide in solid form (~ 2 mg in each case) was taken and mixed with potassium bromide to make up its amount to a level that could be packed properly in the zirconia rotor of 3.2 mm outer diameter. To evaluate the secondary structure of monomeric and aggregated peptide based on the conformation dependent ^{13}C chemical shifts, the ^{13}C CP-MAS [cross-polarization with magic angle spinning] with TOSS (total suppression of spinning side bands) spectra were recorded with a spinning speed of 10 kHz. For cross-polarization, a contact time of 2 ms was used. All of the experiments were recorded using 32 000 transients and a relaxation delay of 6 s.

■ RESULTS AND DISCUSSION

The aggregation of sCT in the presence of metal ions has been demonstrated through a decrease in intensity of resonances in the aliphatic region of ^{1}H NMR spectra (Figure 1) recorded in the solution state at 25 °C (i) just after the addition of metal ions and then (ii) after incubation for 10 days at 37 °C. The intensity variation in the aliphatic region of the sCT peptide with time in the absence as well as in the presence of metal ions (Al^{3+}, Cu^{2+}, and Zn^{2+}) has been displayed in detail (Supporting Information Figures S7–S10). As clear from the figure, a comprehensive reduction in the intensities of ^{1}H resonances

dx.doi.org/10.1021/ic202604v | Inorg. Chem. 2012, 51, 5642–5650

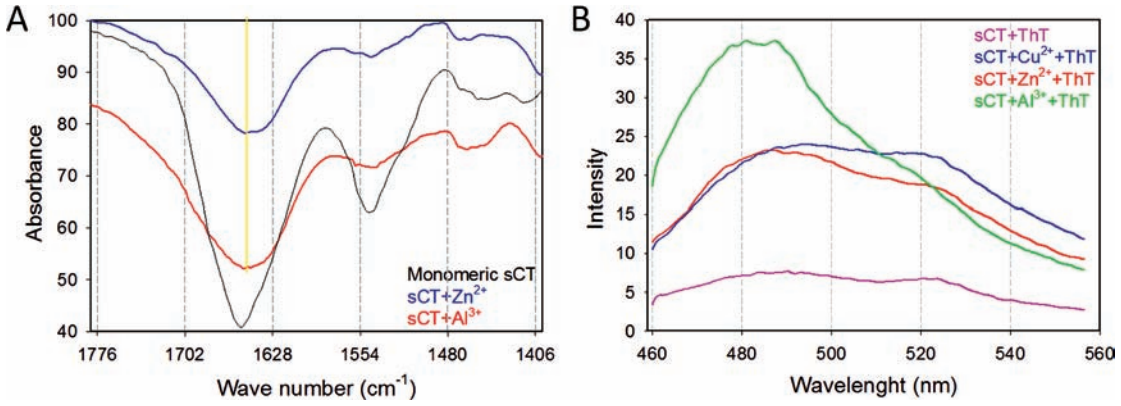

Figure 3. (A) FT-IR spectra of monomeric salmon calcitonin (black) and salmon calcitonin aggregates in the presence of Zn^{2+} ions (blue), and in the presence of Al^{3+} ions (red). (B) Fluorescence emission spectra of thioflavin-T(Th-T) with solutions in the absence (pink) as well as in the presence of metal ions Cu^{2+} (blue), Zn^{2+} (red), and Al^{3+} (green).

was seen with time in the case of sCT peptide treated/agitated with metal ions. This can be attributed to the formation of large molecular assemblies, which results in decreased correlation time of the molecule and hence decreased T_2, causing line broadening. In a metal-free solution, the ^{1}H NMR spectrum of sCT has shown subtle changes in the line width of ^{1}H resonances, which is indicative of nonaggregated conformational transitions of the peptide during the period of incubation. The conformational stability of sCT at a low concentration and ambient temperature has also been proven previously,[44] where it has been shown that the sCT fibrils are formed in a 10 mg/mL solution at 230 °C after nine days. On the basis of these observations, we can say that the presence of metal ions [Cu^{2+}, Zn^{2+}, and Al^{3+}] accelerates/promotes the aggregation process of sCT *in vitro* and hence act as a cofactor for the aggregation process. A point to be noted here is that the copper in the +2 oxidation state is paramagnetic and hence induces additional line broadening in the ^{1}H NMR spectrum recorded just after the addition of Cu^{2+} ions (Figure 1d).

Following these preliminary results of metal ion induced sCT aggregation, the binding of each of these metal ions [Cu^{2+}, Zn^{2+}, and Al^{3+}] with sCT peptide has been investigated on the basis of the amide chemical shift perturbation method. With this aim, we performed the sequence specific assignment of amide (^{1}H and ^{15}N) resonances of sCT in solution (Supporting Information: Appendix I). The poor amide ^{1}H shift dispersion and the absence of inter-amide-proton NOEs in the ^{15}N edited NOESY HSQC spectrum (data not shown) indicated that the peptide is largely unstructured in aqueous solution; the fact has already been reported in several previous studies.[10,13,18,45] After assignment, the HMQC spectra on sCT samples (incubated with metal ions) were recorded to monitor the spectral changes as a consequence of metal ion binding. Specific chemical shift perturbations and broadening of line widths were observed in the [^{1}H−^{15}N]-HSQC spectrum of sCT upon formation of the complex with these metal ions. These changes were observed from the beginning of the titration, when the concentration of sCT/metal ion was ∼1:1 (concentration of sCT in each case was ∼250 μM to prevent the precipitation and nonspecific interactions), until the final concentrations of sCT/metal ion ∼ 1:4 (see Supporting Information: Figures S11 and S12).

Superposition of the HSQC spectra of free sCT and that in complex with metal ions are shown in Figure 2A. For these metal ions, the residues showing most significant perturbations are C1, T6, C7, V8, E15, H17, K18, and L19. These residues can be considered as the main coordination sites. In the case of Cu^{2+} treated sCT solution, the residues C1, S5, T6, C7, V8, E15, and H17 have been broadened beyond the detection limits. Other residues like S2, L12, S13, and T31 have undergone moderate perturbations in their chemical shifts, indicating their lesser affinity toward metal coordination. The intact chemical shifts of sCT amino acid residues during the metal treatment have demonstrated their inertness toward coordination. On the basis of average combined amide chemical shift perturbation (shown in Figure 2B), the main binding sites are located in the N-terminal region from residues C1 to V8 and the central region spanning from E15 to L19. A summary of these results is shown in Figure 2C by mapping the residues undergoing coordination with metal ions (in red) along the primary sequence of salmon calcitonin. Since NMR chemical shifts are highly sensitive toward the local conformational state of the polypeptide chain, the chemical shift perturbations can thus also be due to conformational alterations induced by metal ion binding to the peptide. Thus, it can be speculated that the metal ion coordination and conformational transition are concomitant processes, and this coordination chemistry of calcitonin with metal ions (i.e., Zn^{2+}, Cu^{2+}, and Al^{3+}) may be the key step in inducing the destructive conformational transitions, resulting in an accelerated peptide aggregation process. The results are in good correlation with the role of metal ions investigated in the other amyloidogenic peptides such as hIAPP and β-amyloid.[37,46] In order to confirm that the chemical shift perturbation is a consequence of metal ion coordination to the peptide, an EDTA chelation study was performed on sCT samples with prior incubation (for 2 h at 37 °C) with 1 equivalent of Cu^{2+} and Zn^{2+} ions (prepared separately). Each of these samples was further incubated (for 2 h at 37 °C) with 2 equivalents of EDTA followed by HMQC measurements. The experimental spectra of these two EDTA treated sCT samples have been shown (Supporting Information: Figures S13 and S14) and clearly demonstrate that the amide protons were restored back to their original chemical shifts and reappeared in the case of Cu^{2+}. This recovery of amide resonances to that of sCT in a metal-free solution clearly reinstates coordination of the metal ion to a strong chelating agent, EDTA, indicating the reversible nature of coordination of the metal ions (i.e., Cu^{2+} and Zn^{2+}) with the peptide in aqueous solution. The parallel reversibility of coordination has also been reported in the case of β-amyloid peptide treated with Cu^{2+} and Zn^{2+} ions.[31] The above findings clearly prove that

dx.doi.org/10.1021/ic202604v | *Inorg. Chem.* 2012, 51, 5642−5650

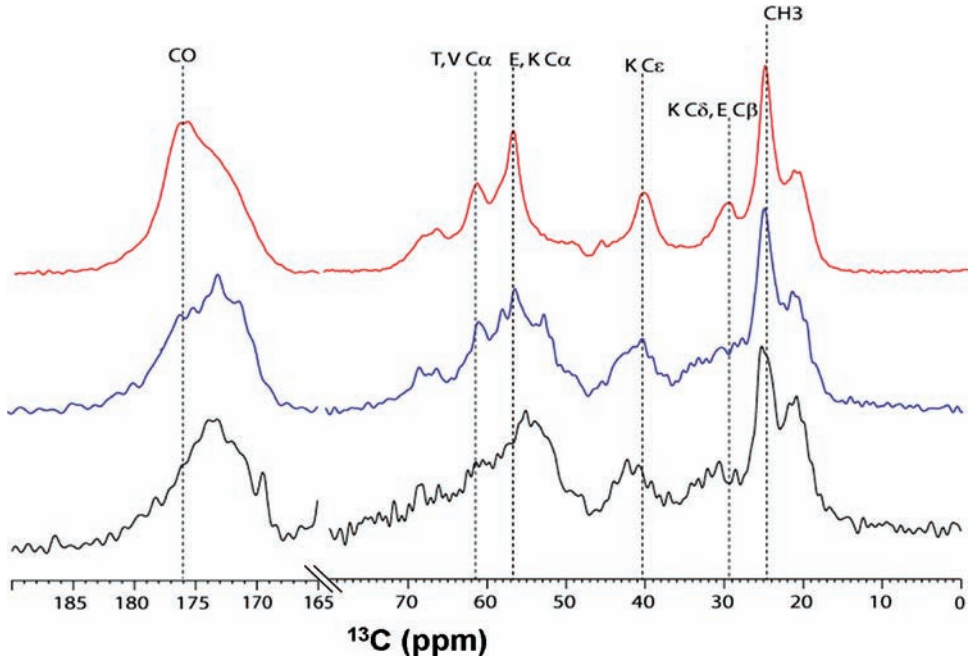

Figure 4. ^{13}C CP-MAS solid state NMR spectra of sCT in the monomeric form (red) and aggregated sCT in the presence of Zn^{2+} (blue) and Al^{3+} (black).

metal ions are interacting with sCT peptide and are inducing conformational transitions, leading to self-association. These initial interesting findings prompted us further to obtain insights into the conformational states of sCT present in these aggregates. In this regard, FT-IR spectroscopy[47,48] has been used, which is known to provide discrimination between secondary structures assumed by peptides directly in the powder/solid state, as revealed by shifting in their amide I bands—corresponding to the carbonyl group of the amide bond—between 1600 and 1700 cm^{-1}.[49,50] The FT-IR experiments were performed on monomeric (before treatment with metal ions) as well as metal induced aggregated sCT samples to derive the information on conformational modulation during the aggregation process. The FT-IR spectrum of metal free sCT (i.e., monomeric sCT sample in its native form) shows a strong amide I band at 1654 cm^{-1} characteristic of a random coil conformation (Figure 3A), whereas sCT aggregates in the presence of Zn^{2+} and Al^{3+} ions show a broad band in the regime from 1650 to 1632 cm^{-1}, emphasizing the turn and β-sheet components.[50]

We have also performed a thioflavin T (ThT) assay (commonly employed for amyloid fibril identification) to demonstrate the aggregation process in the presence of metal ions. In the case of metal treated peptide, a significant enhancement in emission fluorescence of ThT has been observed in comparison to the peptide incubated in the absence of metal ions (Figure 3B). The results are indicative of the presence of a cross-β sheet conformation in the metal treated aggregated peptide. Metal-free peptide with ThT showed insignificant enhancement in the emission fluorescence spectrum, which further reinstates the formation of non-aggregated conformational transitions during the process of incubation as observed in ^{1}H NMR spectroscopy. The higher enhancement in fluorescence emission intensity in the case of Al^{3+} induced aggregated peptide has demonstrated the presence of more ordered amyloid-like cross-β sheet components in comparison to the aggregates induced by other metal ions (Cu^{2+} and Zn^{2+}).

The study was further extended to understand the mechanistic aspects of this aggregation process. The elucidation of the molecular structure of aggregates is an important target for understanding the mechanism of self-aggregation. In order to obtain structural insights into these aggregates, solid-state NMR spectroscopy has proven to be a valuable method.[43] The ^{13}C CP-MAS spectra were recorded for monomeric sCT peptide in the solid form, and for sCT aggregates, they were obtained after incubating with metal ions (here, Zn^{2+} and Al^{3+}). The Cu^{2+} induced peptide aggregates have been excluded from this study due to the paramagnetic nature of the Cu^{2+} ions. The experimental spectra are displayed in Figure 4. The comparison clearly indicates that the carbonyl resonance (at 176.07 ppm for monomer sCT sample) shifted significantly to high field (i.e., upfield shift) in the case of its aggregates obtained with Zn^{2+} and Al^{3+} ions. The upfield shifting of the carbonyl group gives a clear indication of the conformational transition of sCT from a random coil/α-helix to a β-sheet secondary structure.[51] The $^{13}C^{\alpha}$ resonances arising from residues, Thr, Val, Glu, and Lys, are also showing an upfield shift in the case of aggregated peptide. The signals characterizing $^{13}C^{\delta}$ of Lys, $^{13}C^{\beta}$ of Glu, as well as methyl carbons were found to be shifted toward low field. All of this resonance shifting is indicative of conformational transitions toward the β sheet.[52] The β-sheet element in the secondary structure is more pronounced in the case of Al^{3+} induced sCT aggregates, as revealed in the carbonyl region of CP-MAS spectra. Further, the CP-MAS spectra of sCT aggregates formed in the presence of Zn^{2+} and Al^{3+} are clearly different in the 50−70 ppm region as well as in the carbonyl region of the spectra. The differences are suggestive of a different polymorphism assumed by the aggregates possibly due to variation in the mode of association of different geometries of the peptide complex in the presence of two different metal ions. The presence of more resonances in the aliphatic region in the case of aggregates induced by Zn^{2+} compared to Al^{3+} may

dx.doi.org/10.1021/ic202604v | Inorg. Chem. 2012, 51, 5642−5650

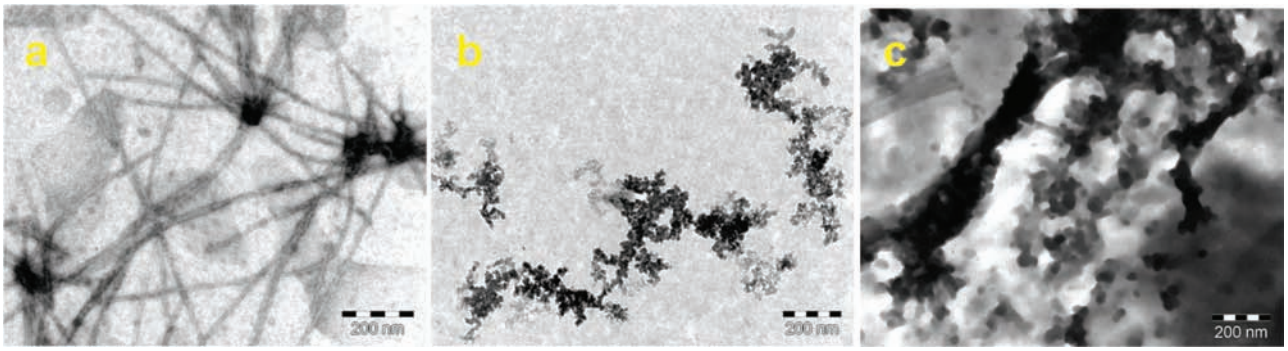

Figure 5. TEM images of sCT solution aged with (a) Al^{3+}, (b) Cu^{2+}, and (c) Zn^{2+} in deionized water at pH 6.5. The scale bar in each panel represents 200 nm. Al^{3+} is efficient in organizing the aggregates into well structured amyloid like fibrillar aggregates. The fibrils are 1−3-μm-long and are of a diameter of ∼15 nm.

be due to the less ordered structure in the former. The carbonyl region in the aggregated peptide in the presence of Zn^{2+} is broader, indicative of a residual random coil component in addition to the converted β sheet. It has been found that intermolecular association occurs when protein fragments with high hydro-phobicity, high β-sheet propensity, and a low net charge are solvent exposed.[53] In the folded state, such aggregation-prone segments are buried, and therefore the protein does not aggregate. However, in the case of unstructured/unfolded peptides/proteins, the hydro-phobic residues remain exposed to the solvent and act as nuclei for aggregation. Thus, aggregation is more facile for intrinsically disordered proteins, and it further accelerates if the peptide/protein has high β-sheet propensity. Several previous studies[54] on amyloidogenic peptides have also revealed this fact that the conformational transitions in these peptides toward the β sheet are responsible for self-association and aggregation. All of these factors nicely correlate with metal ion induced aggregation process of sCT, as it is a highly unstructured peptide, consists of several hydrophobic residues, and metal ion coordination with the peptide induces β-sheet propensity.

The differences in the solid state ^{13}C CP-MAS spectra of aggregates obtained in the presence of Zn^{2+} and Al^{3+} are pointing toward different morphologies attained by peptides in the aggregation process. To probe the morphology of aggregates formed, the sCT samples incubated with metal ions [Cu^{2+}, Zn^{2+}, and Al^{3+}] for 10 days at 37 °C were subjected to TEM analysis. The TEM results were also found to be in good agreement with the 1D ^1H NMR results described above. The TEM images of aged sCT samples incubated for 10 days in the presence of (a) Al^{3+}, (b) Cu^{2+}, and (c) Zn^{2+} are shown in Figure 5 and clearly indicate the formation of aggregates. However, in the case of different metal ions, the morphological variations have been seen in these aggregates, pointing toward different arrangements of monomers during the aggregation. The aqueous sCT solution incubated with Al^{3+} ions has led to the formation of fibrillar aggregates (Figure 5a). The fibrils were characterized to be 1−3-μm-long and of a diameter of ∼15 nm. However, the sCT solution incubated with Cu^{2+} and Zn^{2+} metal ions resulted in globular aggregates, but no fibrillar morphology of aggregates has been observed under these experimental conditions. Similar types of morphological variations of aggregates have also been reported in the case of β-amyloid peptide treated with Zn^{2+} ions.[27] The different morphological features of sCT aggregates formed in the presence of different metal ions clearly suggested that the aggregation process in each case has been mediated through metal binding to the peptide where different metal ions are stabilizing different destructive conformational states of the peptide. The varied conformational states then transform into stabilized aggregates having different morphologies. Further, no aggregate was observed in the case of agitated sCT solution for 10 days in the absence of any metal ion, indicating that the aggregation of sCT peptide in solution is rather a slow process, like has been reported previously.[15]

■ CONCLUDING REMARKS

In conclusion, we report here the metal ion (Cu^{2+}, Zn^{2+}, Al^{3+}) interaction with sCT peptide in an aqueous environment and then the characterization of sCT aggregates formed in the presence of these multivalent metal ions using various biophysical techniques: NMR (both solution state and solid state), TEM, FT-IR, and ThT fluorescence assay. The ^1H NMR experiments revealed that the metal ions (Cu^{2+}, Zn^{2+}, Al^{3+}) act as cofactors to accelerate the aggregation of sCT peptide (at the therapeutically used concentration of ∼250 μM and near physiological pH of 6.5). Similar results have also been observed for peptide—β-amyloid—treated with Fe^{2+} ions.[25] Next, the NMR chemical shift perturbation method was used to evaluate the metal ion binding to the peptide and leading to conformational transitions. These conformational transitions occurring on coordination with the metal ion have been anticipated as the key factor in the aggregation process. In striking contrast with bivalent metal ions (Cu^{2+} and Zn^{2+}), the trivalent metal ion Al^{3+} strongly stimulates the conversion of monomer peptide into fibrillar aggregates in aqueous solution. The reversibility of coordination of metal ions Cu^{2+} and Zn^{2+} as well as the capability of Zn^{2+} to inhibit the fibrillar morphology of aggregates points toward a close resemblance in the metal induced aggregation phenomenon of both β-amyloid and sCT peptides. We believe that the results presented here will give a new direction to increase the therapeutic potency of salmon calcitonin in aqueous solution.

■ ASSOCIATED CONTENT

Ⓢ Supporting Information

The strategy employed for backbone amide assignment of sCT. This information is available free of charge via the Internet at http://pubs.acs.org.

dx.doi.org/10.1021/ic202604v | Inorg. Chem. 2012, 51, 5642−5650

AUTHOR INFORMATION

Corresponding Author

*Corresponding Author: Prof. Raja Roy Centre of Biomedical Magnetic Resonance (CBMR), SGPGIMS Campus, Raibareli Road, Lucknow-226014, Uttar Pradesh, India Email: rajaroy28@gmail.com; roy@cbmr.res.in .Phone: +91-9005095427.

Notes

The authors declare no competing financial interest.

ACKNOWLEDGMENTS

We gratefully acknowledge Dr. T. Rajamannar, Director, Sun Pharma Advance Research Company Ltd., Baroda, Gujrat, India for providing pure sCT as a gift for our study. We thank to Prof. C. L. Khetrapal for his kind support throughout this work. We also acknowledge Dr. Ashish Arora, CDRI, Lucknow for his kind help in Tht-fluorescence experiments. N.R. is also thankful to CSIR for fellowship.

ABBREVIATIONS

TEM, Transmission Electron Microscopy; AD, Alzheimer's Disease; sCT, Salmon Calcitonin; FT-IR, Fourier Transform Infra Red Spectroscopy; CP-MAS, Cross-Polarization Magic Angle Spinning

REFERENCES

(1) Copp, D. H.; Cheney, B. *Nature* **1962**, *193*, 381−382.
(2) Copp, D. H. *Mod. Treat.* **1970**, *7* (3), 621−635.
(3) Gaudiano, M. C.; Colone, M.; Bombelli, C.; Chistolini, P.; Valvo, L.; Diociaiuti, M. *Biochim. Biophys. Acta* **2005**, *1750* (2), 134−145.
(4) Mehta, N. M.; Malootian, A.; Gilligan, J. P. *Curr. Pharm. Des* **2003**, *9* (32), 2659−2676.
(5) Schneider, D.; Hofmann, M. T.; Peterson, J. A. *Am. Fam. Physician* **2002**, *65* (10), 2069−2072.
(6) Silverman, S. L. *Am. J. Med. Sci.* **1997**, *313* (1), 13−16.
(7) Abedini, A.; Raleigh, D. P. *Protein Eng. Des. Sel.* **2009**, *22* (8), 453−459.
(8) Diociaiuti, M.; Polzi, L. Z.; Valvo, L.; Malchiodi-Albedi, F.; Bombelli, C.; Gaudiano, M. C. *Biophys. J.* **2006**, *91* (6), 2275−2281.
(9) Moriarty, D. F.; Vagts, S.; Raleigh, D. P. *Biochem. Biophys. Res. Commun.* **1998**, *245* (2), 344−348.
(10) Amodeo, P.; Motta, A.; Strazzullo, G.; Castiglione Morelli, M. A. *J. Biomol. NMR* **1999**, *13* (2), 161−174.
(11) Khurana, R.; Agarwal, A.; Bajpai, V. K.; Verma, N.; Sharma, A. K.; Gupta, R. P.; Madhusudan, K. P. *Endocrinology* **2004**, *145* (12), 5465−5470.
(12) Fowler, S. B.; Poon, S.; Muff, R.; Chiti, F.; Dobson, C. M.; Zurdo, J. *Proc. Natl. Acad. Sci. U. S. A* **2005**, *102* (29), 10105−10110.
(13) Azria, M.; Copp, D. H.; Zanelli, J. M. *Calcif. Tissue Int.* **1995**, *57* (6), 405−408.
(14) Gaudiano, M. C.; Diociaiuti, M.; Bertocchi, P.; Valvo, L. *Biochim. Biophys. Acta* **2003**, *1623* (1), 33−40.
(15) Arvinte, T.; Cudd, A.; Drake, A. F. *J. Biol. Chem.* **1993**, *268* (9), 6415−6422.
(16) Breydo, L.; Uversky, V. N. *Metallomics* **2011**, *3*, 1163−1180.
(17) Meadows, R. P.; Nikonowicz, E. P.; Jones, C. R.; Bastian, J. W.; Gorenstein, D. G. *Biochemistry* **1991**, *30* (5), 1247−1254.
(18) Arvinte, T.; Drake, A. F. *J. Biol. Chem.* **1993**, *268* (9), 6408−6414.
(19) Zagorski, M. G.; Yang, J.; Shao, H.; Ma, K.; Zeng, H.; Hong, A. *Methods Enzymol.* **1999**, *309*, 189−204.
(20) Ma, K.; Clancy, E. L.; Zhang, Y.; Ray, D. G.; Wollenberg, K.; Zagorski, M. G. *J. Am. Chem. Soc.* **1999**, *121* (38), 8698−8706.
(21) Messerschmidt, A.; Huber, R.; Wieghardt, K.; Poulos, T. *Handbook of Metalloproteins*; Wiley Online Library: Hoboken, NJ, 2001.
(22) Mantyh, P. W.; Ghilardi, J. R.; Rogers, S.; DeMaster, E.; Allen, C. J.; Stimson, E. R.; Maggio, J. E. *J. Neurochem.* **1993**, *61* (3), 1171−1174.
(23) Zatta, P.; Drago, D.; Bolognin, S.; Sensi, S. L. *Trends Pharmacol. Sci.* **2009**, *30* (7), 346−355.
(24) Ryu, J.; Girigoswami, K.; Ha, C.; Ku, S. H.; Park, C. B. *Biochemistry* **2008**, *47* (19), 5328−5335.
(25) Bousejra-ElGarah, F.; Bijani, C.; Coppel, Y.; Faller, P.; Hureau, C. *Inorg. Chem.* **2011**, *50* (18), 9024−9030.
(26) Bolognin, S.; Messori, L.; Zatta, P. *Neuromol. Med.* **2009**, *11* (4), 223−238.
(27) Noy, D.; Solomonov, I.; Sinkevich, O.; Arad, T.; Kjaer, K.; Sagi, I. *J. Am. Chem. Soc.* **2008**, *130* (4), 1376−1383.
(28) Miller, Y.; Ma, B.; Nussinov, R. *Proc. Natl. Acad. Sci. U. S. A.* **2010**, *107* (21), 9490−9495.
(29) Moir, R. D.; Atwood, C. S.; Huang, X.; Tanzi, R. E.; Bush, A. I. *Eur. J. Clin. Invest.* **1999**, *29* (7), 569−570.
(30) Lee, J. S.; Ryu, J.; Park, C. B. *Anal. Chem.* **2009**, *81* (7), 2751−2759.
(31) Hou, L.; Zagorski, M. G. *J. Am. Chem. Soc.* **2006**, *128* (29), 9260−9261.
(32) Hindo, S. S.; Mancino, A. M.; Braymer, J. J.; Liu, Y.; Vivekanandan, S.; Ramamoorthy, A.; Lim, M. H. *J. Am. Chem. Soc.* **2009**, *131* (46), 16663−16665.
(33) Valensin, D.; Migliorini, C.; Valensin, G.; Gaggelli, E.; La, P. G.; Kozlowski, H.; Gabbiani, C.; Messori, L. *Inorg. Chem.* **2011**, *50* (15), 6865−6867.
(34) Brender, J. R.; Hartman, K.; Nanga, R. P.; Popovych, N.; de la Salud, B. R.; Vivekanandan, S.; Marsh, E. N.; Ramamoorthy, A. *J. Am. Chem. Soc.* **2010**, *132* (26), 8973−8983.
(35) Salamekh, S.; Brender, J. R.; Hyung, S. J.; Nanga, R. P.; Vivekanandan, S.; Ruotolo, B. T.; Ramamoorthy, A. *J. Mol. Biol.* **2011**, *410* (2), 294−306.
(36) Brender, J. R.; Salamekh, S.; Ramamoorthy, A. *Acc. Chem. Res.* **2012**, *45* (3), 454−462.
(37) DeToma, A. S.; Salamekh, S.; Ramamoorthy, A.; Lim, M. H. *Chem. Soc. Rev.* **2012**, *41* (2), 608−621.
(38) Huang, R.; Vivekanandan, S.; Brender, J. R.; Abe, Y.; Naito, A.; Ramamoorthy, A. *J. Mol. Biol.* **2012**, *416* (1), 108−120.
(39) Schanda, P.; Kupce, E.; Brutscher, B. *J. Biomol. NMR* **2005**, *33* (4), 199−211.
(40) Cavanagh, J.; Fairbrother, W. J.; Palmer, A. G.; Skelton, N. J. *Protein NMR spectroscopy principles and practice*; Academic Press: San Diego, CA, 1996.
(41) *The Computer Aided Resonance Assignment Tutorial CANTINA*, Verlag: Goldau, Switzerland, 2004.
(42) Yamamoto, K.; Vivekanandan, S.; Ramamoorthy, A. *J. Phys. Chem B* **2011**, *115* (43), 12448−12455.
(43) Kamihira, M.; Naito, A.; Tuzi, S.; Nosaka, A. Y.; Saito, H. *Protein Sci.* **2000**, *9* (5), 867−877.
(44) Gilchrist, P. J.; Bradshaw, J. P. *Biochim. Biophys. Acta* **1993**, *1182* (1), 111−114.
(45) Epand, R. M.; Epand, R. F.; Orlowski, R. C.; Seyler, J. K.; Colescott, R. L. *Biochemistry* **1986**, *25* (8), 1964−1968.
(46) Brender, J. R.; Hartman, K.; Nanga, R. P.; Popovych, N.; de la Salud, B. R.; Vivekanandan, S.; Marsh, E. N.; Ramamoorthy, A. *J. Am. Chem. Soc.* **2010**, *132* (26), 8973−8983.
(47) Dzwolak, W.; Smirnovas, V. *Biophys. Chem* **2005**, *115* (1), 49−54.
(48) Okuno, A.; Kato, M.; Taniguchi, Y. *Biochim. Biophys. Acta* **2007**, *1774* (5), 652−660.
(49) Bauer, H. H.; Muller, M.; Goette, J.; Merkle, H. P.; Fringeli, U. P. *Biochemistry* **1994**, *33* (40), 12276−12282.
(50) Beekes, M.; Lasch, P.; Naumann, D. *Vet. Microbiol.* **2007**, *123* (4), 305−319.

(51) Kim, H. Y.; Cho, M. K.; Kumar, A.; Maier, E.; Siebenhaar, C.; Becker, S.; Fernandez, C. O.; Lashuel, H. A.; Benz, R.; Lange, A.; Zweckstetter, M. *J. Am. Chem. Soc.* **2009**, *131* (47), 17482−17489.
(52) Kamihira, M.; Naito, A.; Tuzi, S.; Nosaka, A. Y.; Saito, H. *Protein Sci.* **2000**, *9* (5), 867−877.
(53) Burkoth, T. S.; Benzinger, T. L. S.; Urban, V.; Morgan, D. M.; Gregory, D. M.; Thiyagarajan, P.; Botto, R. E.; Meredith, S. C.; Lynn, D. G. *J. Am. Chem. Soc.* **2000**, *122* (33), 7883−7889.
(54) Garvey, M.; Tepper, K.; Haupt, C.; Knupfer, U.; Klement, K.; Meinhardt, J.; Horn, U.; Balbach, J.; Fandrich, M. *Biochem. Biophys. Res. Commun.* **2011**, *409* (3), 385−388.